JACS
JOURNAL OF THE AMERICAN CHEMICAL SOCIETY

Communication

pubs.acs.org/JACS

Homochiral 2D Porous Covalent Organic Frameworks for Heterogeneous Asymmetric Catalysis

Xiuren Wang,[†,§] Xing Han,[†,§] Jie Zhang,[†] Xiaowei Wu,[†] Yan Liu,*[,†] and Yong Cui*[,†,‡]

[†]School of Chemistry and Chemical Engineering and State Key Laboratory of Metal Matrix Composites, Shanghai Jiao Tong University, Shanghai 200240, China

[‡]Collaborative Innovation Center of Chemical Science and Engineering, Tianjin 300072, China

Supporting Information

ABSTRACT: There have been breakthroughs in the development of covalent organic frameworks (COFs) with tunability of composition, structure, and function, but the synthesis of chiral COFs remains a great challenge. Here we report the construction of two-dimensional COFs with chiral functionalities embedded into the frameworks by imine condensations of enantiopure TADDOL-derived tetraaldehydes with 4,4′-diaminodiphenylmethane. Powder X-ray diffraction and computer modeling together with pore size distribution analysis show that one COF has a twofold-interpenetrated grid-type network and the other has a non-interpenetrated grid network. After postsynthetic modification of the chiral dihydroxy groups of TADDOL units with $Ti(O^iPr)_4$, the materials are efficient and recyclable heterogeneous catalysts for asymmetric addition of diethylzinc to aldehydes with high enantioselectivity. The results reported here will greatly expand the scope of materials design and engineering for the creation of new types of functional porous materials.

Covalent organic frameworks (COFs), formed by connecting multidentate organic building blocks through covalent bonds, represent an emerging class of porous crystalline materials with tunability of composition, structure, and function.[1−3] Numerous COFs have been prepared using different linkages such as boronate,[1] boroxine,[1] imine,[2a,b] and hydrazone,[2c] and some of them have been explored for potential applications such as gas storage and separation,[4,5] optoelectronics,[6] energy storage,[7] drug delivery,[8] sensing,[3b,9] and catalysis.[10,11] Like metal−organic frameworks (MOFs),[12] COFs are typically crystallized under mild conditions, which may allow the construction of chiral COFs (CCOFs) by judicious choices of enantiopure building blocks or templates. Chiral porous materials are of particular interest because of the increasing demand for materials for asymmetic catalysis and separation and fundamental aspects in chirality.[13] However, it remains a major challenge to make CCOFs because of the difficulty in controlling the crystallization of pure covalent organic materials, especially in optically pure forms.[11,14] In fact, only several COFs functionalized with (+)-diacetyl-L-tartaric anhydride and (*S*)-pyrrolidine have been prepared by direct or postsynthetic synthesis approaches.[11] In all cases, the chiral functionalities dangle from the framework rather than being embedded in it, and they do not have a high level of synergism with the networks.

Two-dimensional (2D) COFs could be realized by combining virtually planar building units into extended sheets, which pack via dispersive forces into anisotropic crystalline materials.[15] It is believed that the control of intralayer interactions and layer planarity via the introduction of hydrogen bonds that allow for constant self-healing during crystal growth could induce and even improve the crystallinity of layered COFs.[16] Tetraaryl-1,3-dioxolane-4,5-dimethanols (TADDOLs), versatile chiral auxiliaries and privileged ligands for asymmetric catalysis, are tartaric acid derivatives with four aryl substituents in a propeller type conformation.[17] In addition to the 1,3-dioxolane structure, they also possess a 1,4-diol moiety, one hydrogen atom of which is involved in an intramolecular hydrogen bond while the other is free for intermolecular interactions, thereby providing structures with a fair amount of rigidity. We surmised that a tetraaldehyde-functionalized TADDOL derivative might be an intriguing 2D COF building block because of its strong hydrogen-bonding ability and a parallelogram arrangement of the coplanar aldehyde groups associated with a semirigid backbone. It should be noted that the propeller-like conformation of building blocks has been utilized as a self-repeating docking site for the attachment of consecutive COF layers to promote crystal growth.[18] Here we report the synthesis of two 2D porous CCOFs by imine condensations of enantiopure TADDOL-derived tetraaldehydes with 4,4′-diaminodiphenylmethane (4,4′-DADPM), which, after treatment with $Ti(O^iPr)_4$, are efficient heterogeneous catalysts for the asymmetric addition of diethylzinc to aldehydes.

CCOF-**1** and CCOF-**2** were synthesized by solvothermal reactions of enantiopure TTA or TTPA (0.25 mmol) and 4,4′-DADPM (0.5 mmol) in 1,4-dioxane (6 mL) and 9 M aqueous acetic acid (1.5 mL) at 100 °C for 3 days, which afforded gray microcrystalline solids in yields of about 70% (Scheme 1). The CCOFs are stable in common organic solvents. The as-synthesized CCOFs were characterized by Fourier transform infrared (FT-IR) spectroscopy. The spectra of **1** and **2** show the nearly complete disappearance of the characteristic C═O stretching band (1702 cm^{-1}), indicating that the free aldehydes were mostly consumed. Strong stretching vibration bands at 1624 and 1623 cm^{-1} were detected for CCOF-**1** and CCOF-**2**, respectively, suggesting the formation of C═N linkages (Figure S1).

The ^{13}C cross-polarization magic-angle spinning NMR spectrum shows the characteristic signal for the C═N group

Received: July 26, 2016
Published: September 13, 2016

DOI: 10.1021/jacs.6b07714
J. Am. Chem. Soc. 2016, 138, 12332−12335

Scheme 1. Synthesis of the CCOFs

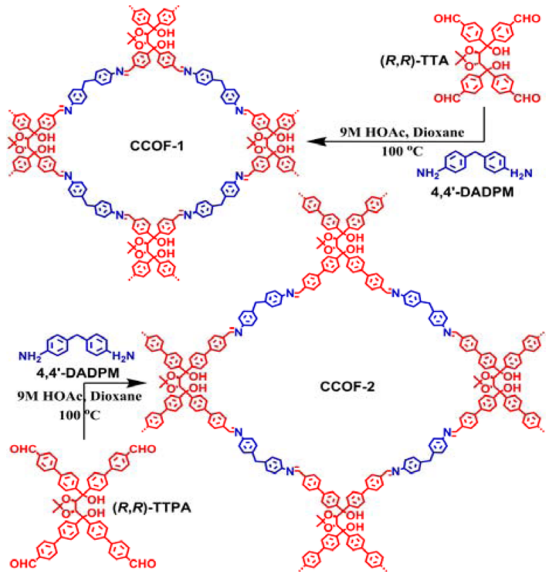

at about 158 and 157 ppm for CCOF-**1** and CCOF-**2**, respectively (Figure S2). The aldehyde carbon peaks were barely observed. The chemical shifts of other fragments are in good agreement with those of the monomers. Circular dichroism (CD) spectra of CCOF-**1** and CCOF-**2** made from the (*R*,*R*) and (*S*,*S*) enantiomers of the TADDOL monomers are mirror images of each other, indicative of their enantiomeric nature (Figure S4). Thermogravimetric analysis (TGA) revealed that they both are stable up to around 380 °C (Figure S5). Scanning electron microscopy (SEM) images showed that both of the CCOFs were aggregates of sheetlike structures. The 2D nature of the frameworks was indicated by transmission electron microscopy (TEM) characterizations (Figure S6).

The crystalline structures of the two CCOFs were determined by powder X-ray diffraction (PXRD) analysis with Cu Kα radiation (Figure 1). Several types of possible 2D structures were generated for them, that is, single-pore (sp), dual-pore (dp), and triple-pore (tp) structures. For each type of structure, eclipsed stacking (AA) and staggered stacking (AB) were constructed. After geometrical energy minimizations based on the parallel twofold-interpenetrated 2D net with the AB stacking mode for CCOF-**1** and the non-interpenetrated 2D net with the AB stacking mode for CCOF-**2**, the unit cell parameters were obtained (a = 37.42 Å, b = 37.42 Å, c = 8.23 Å, α = 90°, β = 89.49°, and γ = 90° for CCOF-**1**; a = 48.14 Å, b = 48.14 Å, c = 29.85 Å, and $\alpha = \beta = \gamma$ = 90° for CCOF-**2**). The experimental PXRD pattern for CCOF-**1** (Figure 1a, black curve) shows the main diffraction peaks at 6.67°, 10.65°, 13.43°, and 14.39°, corresponding to the (220), (001), (440), and (041) facets of space group $P2_1$ (No. 4), respectively. This PXRD pattern was in good agreement with the simulated pattern based on the twofold-interpenetrated sp structure of CCOF-**1** (Figure 1a, blue curve), suggesting that the material holds a single-pore structure with the AB stacking model. Lattice modeling and Pawley refinement (Materials Studio, version 7.0) gave optimized parameters of a = 37.41 Å, b = 37.11 Å, c = 8.20 Å, α = 90.0°, β = 89.11°, and γ = 90.0° for the unit cell with space group $P2_1$, which provided two good agreement factors (R_p = 5.82% and R_{wp} = 6.97%).

The experimental PXRD pattern for CCOF-**2** (Figure 1b, black curve) with space group $P2_1$ (No. 4) exhibited peaks at

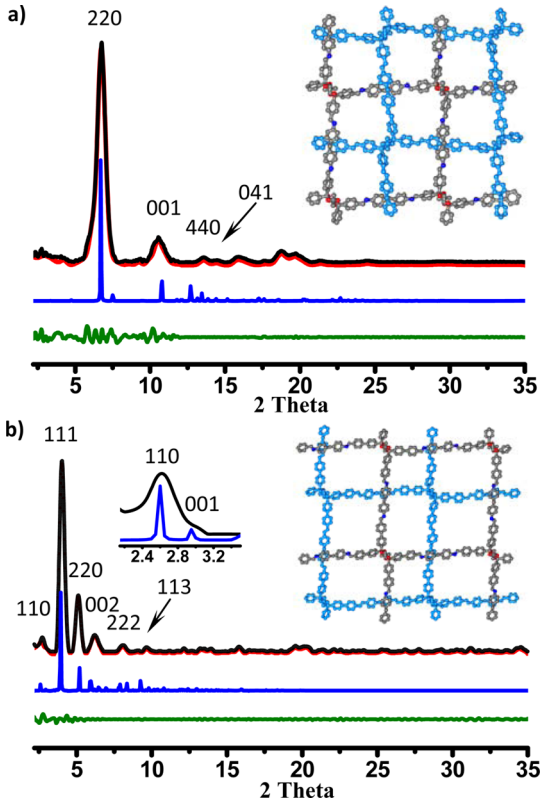

Figure 1. PXRD patterns of (a) CCOF-**1** and (b) CCOF-**2** with the experimental profiles in black, Pawley-refined profiles in red, calculated profiles in blue, and the differences between the experimental and refined PXRD patterns in dark green. Inset in (a): parallel twofold-interpenetrated layers of **1**. Insets in (b): (left) 110 and 001 facets and (right) AB stacking layers of **2**.

2.59°, 2.96°, 3.95°, 5.20°, 5.93°, 7.90°, and 9.27°, which were assigned to the (110), (001), (111), (220), (002), (222), and (113) facets, respectively. This PXRD pattern was in good agreement with the simulated pattern based on the non-interpenetrated tp structure (Figure 1b, blue curve), suggesting that the framework has a triple similar pore structure with the AB stacking model. The refinement results yielded unit cell parameters nearly equivalent to the predictions (a = 48.14 Å, b = 48.08 Å, c = 29.85 Å, α = 90°, β = 90.24°, and γ = 90°) with acceptably low residuals (R_p = 3.03% and R_{wp} = 4.25%). PXRD patterns were also calculated for the two CCOFs on the other structures, but the calculated PXRD patterns did not match the experimental patterns well (Figures S11 and S13). Moreover, CCOF-**1** with an sp structure in AB stacking mode and CCOF-**2** with a tp structure in AB stacking mode were found to have much lower total energies (636.6 and 878.8 kcal/mol, respectively) than those calculated for other types stacking models (Figures S10 and S12), indicating that the simulated structure is energetically more favored.

The two CCOFs are therefore proposed to have the architectures shown in Figure 2. The propeller-like configuration of the TADDOL units in combination with the angular nature of 4,4′-DADPM thus allows the formation of a corrugated sheet network lying in the *ab* plane with 1D open channels of 9.7 Å for CCOF-**1** and 7−11 Å for CCOF-**2**. Such grids stack along the *c* axis via interdigitation of the TADDOL rings from the adjacent layers, with shortest and longest interlayer separations of 3.25 and 8.2 Å for CCOF-**1** and 3.32 and 29.8 Å for CCOF-**2**,

DOI: 10.1021/jacs.6b07714
J. Am. Chem. Soc. 2016, 138, 12332−12335

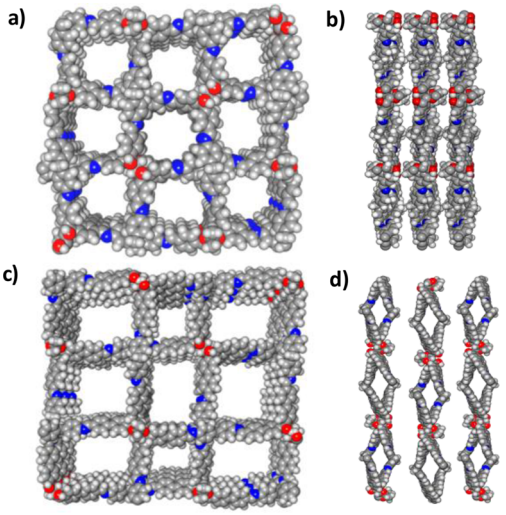

Figure 2. Views of space-filling models of (a, b) CCOF-**1** and (c, d) CCOF-**2** along the (a, c) *c* axis and (b, d) *b* axis.

respectively. In the PXRD patterns, peaks at 10.76° for CCOF-**1** and 2.96° for CCOF-**2** correlating to the values of the interlayer distances were observed. The *d* spacings for them were calculated to be 8.2 and 29.8 Å, respectively.

The porosity of the CCOFs was examined by measuring N_2 adsorption−desorption isotherms at 77 K on the activated samples (Figure 3). The Brunauer−Emmett−Teller (BET)

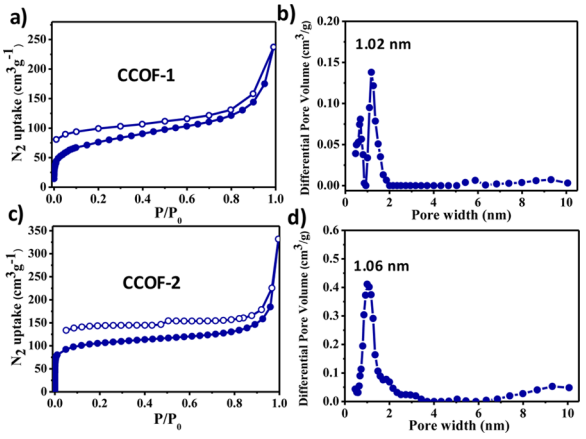

Figure 3. (a, c) N_2 adsorption−desorption isotherms at 77 K and (b, d) pore size distribution profiles for (a, b) CCOF-**1** and (c, d) CCOF-**2**.

surface areas of CCOF-**1** and CCOF-**2** were found to be 266 and 335 m^2g^{-1}, respectively. Their total pore volumes were calculated to be 0.32 and 0.51 $cm^3\ g^{-1}$, respectively, at P/P_0 = 0.99. Nonlocal density functional theory (NLDFT) gave rise to narrow pore size distributions with average pore widths of 10.2 Å for **1** and 10.6 Å for **2**, corresponding to their simulated values (9.7 Å for **1** and 7−11 Å for **2**). The observed hysteresis may be attributed to the dynamic response of the flexible framework, which was found in some microporous 2D or 3D COFs.[2b,10a] The measured surface areas are much smaller than the calculated values of 2224 and 4005 $m^2\ g^{-1}$ for **1** and **2**, respectively, presumably because of incomplete removal of some unreacted monomers and/or solvent molecules in the pores and possible framework distortion upon activation (Figure S7c,d), as observed in some other COFs[19a] and flexible MOFs.[19b] The framework flexibility of the two CCOFs may arise from the flexible 4,4′-DADPM building blocks and semirigid TTA or TTPA units. Notably, most of the reported COFs are based on rigid building blocks.[1,2]

We employed the CCOFs for heterogeneous asymmetric catalysis by taking advantage of their chiral dihydroxy groups. $Ti(O^iPr)_4$ reacts with the dihydroxy groups of TADDOL or its derivatives to give Lewis acidic (TADDOLate)$Ti(O^iPr)_2$ compounds, which are efficient catalysts for the addition of Et_2Zn to aromatic aldehydes to produce enantiopure secondary alcohols.[17] After optimization of the reaction conditions, CCOF-**1** in the presence of excess $Ti(O^iPr)_4$ was found to be an active catalyst for the addition reaction.[17a] Especially, the addition of Et_2Zn to benzaldehyde was carried out in toluene solution in the presence of 20 mol % CCOF-**1** and 3.0 equiv of $Ti(O^iPr)_4$ (the excess $Ti(O^iPr)_4$ was removed in vacuo) at −30 °C for 10 h, affording 1-phenyl-1-propanol with 99% conversion and 90% ee (Table 1, entry 1). Aromatic aldehydes bearing electron-donating and electron-withdrawing groups were converted to the products in >94% conversion with >90% ee (Table 1, entries 3 and 5). The catalytic reaction also worked well with the vinyl-type aromatic aldehyde cinnamaldehyde, affording the product with 91% ee. High enantioselectivity was attained with 2-naphthaldehyde, which afforded 96% conversion and 94% ee. For the bulky substrate 1-pyrenylaldehyde, 97% conversion and 82% ee were obtained.

Table 1. Addition of Diethylzinc to Aromatic Aldehydes Catalyzed by CCOF/Ti[a,b]

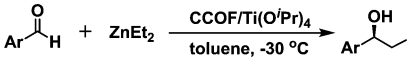

entry[a]	CCOF	Ar	conv (%)[c]	ee (%)[d]
1	**1**	C_6H_5	99 (99)[e]	90 (90)[e]
2	**2**	C_6H_5	99	85
3	**1**	*p*-MeC_6H_4	99 (99)[e]	93 (86)[e]
4	**2**	*p*-MeC_6H_4	99	88
5	**1**	*p*-ClC_6H_5	94 (99)[e]	90 (87)[e]
6	**2**	*p*-ClC_6H_5	96	86
7	**1**	$C_6H_5C{=}CH$	99 (99)[e]	91 (89)[e]
8	**2**	$C_6H_5C{=}CH$	99	85
9	**1**	2-naphthyl	96 (99)[e]	94 (93)[e]
10	**2**	2-naphthyl	96	95
11	**1**	1-pyrenyl	97 (99)[e]	82 (78)[e]
12	**2**	1-pyrenyl	96	74
13	**1**	coronenyl	<5 (64)[e]	n.d.
14	**2**	coronenyl	<5	n.d.

[a]All reactions were carried out with stirring for 10 h at −30 °C using 20 mol % CCOF catalyst with excess $Ti(O^iPr)_4$ (3.0 equiv) and Et_2Zn (2.0 equiv). [b]A comparison with different heterogeneous catalysts in the addition of Et_2Zn to aromatic aldehydes is given in Table S1. [c]Calculated by ^1H NMR analysis. [d]Determined by HPLC. [e]20 mol % TADDOL with excess $Ti(O^iPr)_4$ (3.0 equiv) was used as a homogeneous catalyst.

Under otherwise identical conditions, CCOF-**2** could also catalyze the Et_2Zn addition reactions with catalytic activities and enantioselectivities similar to those of CCOF-**1**. As shown in Table 1, CCOF-**1** displayed enantioselectivities comparable to those of its homogeneous control for the examined substrates as well. Notably, TADDOLs have been immobilized on diverse supports such as resin, dendrimers, amorphous porous organic polymers, and mesoporous silica, but these catalysts in general

DOI: 10.1021/jacs.6b07714
J. Am. Chem. Soc. 2016, 138, 12332−12335

suffer from the disadvantages of fewer and uneven catalytic sites.[20−22] For the diethylzinc addition reaction, the enantioselectivities observed for CCOF-**1** are comparable to or higher than those of reported TADDOL-POP-derived catalysts[22,23] and are higher than those of chiral BINOL−MOF-derived catalysts (Table S1).[24]

We also demonstrated the heterogeneity and recyclability of the CCOF catalysts. First, the supernatant obtained from the diethylzinc addition to benzaldehyde did not afford any additional product. Second, upon completion of the reaction, the catalysts could be readily recovered and used repeatedly without loss of activity for the following four runs (>96% conversion and 90/85, 90/85 89/83, 88/83, and 88/83% ee for runs 1−5 with CCOF-**1**/CCOF-**2**, respectively). After five cycles, PXRD indicated that the solid catalysts remained crystalline but that the structures became seriously distorted (Figure S8). Third, when coronenyl aldehyde, a sterically more demanding substrate with a molecular size of ∼11.1 Å × 13.8 Å, was subjected to the reaction, less than 5% conversions were detected with the CCOF/Ti catalysts (Table 1, entries 13 and 14). The conversions were much lower than the 64% conversion obtained with TADDOL/Ti, probably because this bulky substrate cannot reach the internal catalytic centers via the open channels, indicating that the catalytic reactions for other aldehydes (molecular sizes <9.8 Å × 9.7 Å) mainly occur within the CCOFs.

In summary, we have synthesized two 2D imine-based CCOFs from enantiopure TADDOL-derived tetraaldehydes and a flexible diamine linker. The materials were characterized by a variety of techniques, and their crystal structures were determined by PXRD and computer modeling. After functionalization with $Ti(O^iPr)_4$, the solids could serve as Lewis acid catalysts for the asymmetric addition of diethylzinc to aromatic aldehydes with up to 99% conversion and 95% ee. The heterogeneous catalysts can be recycled and reused without any apparent loss of catalytic activity and enantioselectivity. This work therefore not only demonstrates that it is possible to design and synthesize CCOFs with permanent porosity from enantiopure organic units but also shows that the modular synthetic approach based on chiral building blocks promises to produce a variety of COF materials for practically useful enantioselective processes.

■ ASSOCIATED CONTENT

Supporting Information

The Supporting Information is available free of charge on the ACS Publications website at DOI: 10.1021/jacs.6b07714.

Procedures and characterization data (PDF)

■ AUTHOR INFORMATION

Corresponding Authors

*yongcui@sjtu.edu.cn

*liuy@sjtu.edu.cn

Author Contributions

§X.W. and X.H. contributed equally.

Notes

The authors declare no competing financial interest.

■ ACKNOWLEDGMENTS

This work was financially supported by the NSFC (21371119, 21431004, 21401128, 21522104, and 21620102001), the 973 Program (2014CB932102, 2012CB8217, and 2016YFA0203400), and the "Eastern Scholar" Program.

■ REFERENCES

(1) Côte, A. P.; Benin, A. I.; Ockwig, N. W.; O'Keeffe, M.; Matzger, A. J.; Yaghi, O. M. *Science* **2005**, *310*, 1166.

(2) (a) Kandambeth, S.; Mallick, A.; Lukose, B.; Mane, M.; Heine, T.; Banerjee, R. *J. Am. Chem. Soc.* **2012**, *134*, 19524. (b) Uribe-Romo, F. J.; Hunt, J. R.; Furukawa, H.; Klöck, C.; O'Keeffe, M.; Yaghi, O. M. *J. Am. Chem. Soc.* **2009**, *131*, 4570. (c) Bunck, D. N.; Dichtel, W. R. *J. Am. Chem. Soc.* **2013**, *135*, 14952.

(3) (a) Spitler, E. L.; Dichtel, W. R. *Nat. Chem.* **2010**, *2*, 672. (b) Fang, Q.; Zhuang, Z.; Gu, S.; Kaspar, R. B.; Zheng, J.; Wang, J.; Qiu, S.; Yan, Y. *Nat. Commun.* **2014**, *5*, 4503. (c) Beaudoin, D.; Maris, T.; Wuest, J. D. *Nat. Chem.* **2013**, *5*, 830.

(4) (a) Han, S. S.; Furukawa, H.; Yaghi, O. M.; Goddard, W. A. *J. Am. Chem. Soc.* **2008**, *130*, 11580. (b) Zeng, Y.; Zou, R.; Luo, Z.; Zhang, H.; Yao, X.; Ma, X.; Zou, R.; Zhao, Y. *J. Am. Chem. Soc.* **2015**, *137*, 1020.

(5) (a) Oh, H.; Kalidindi, S. B.; Um, Y.; Bureekaew, S.; Schmid, R.; Fischer, R. A.; Hirscher, M. *Angew. Chem., Int. Ed.* **2013**, *52*, 13219. (b) Ma, H.; Ren, H.; Meng, S.; Yan, Z.; Zhao, H.; Sun, F.; Zhu, G. *Chem. Commun.* **2013**, *49*, 9773.

(6) Wan, S.; Guo, J.; Kim, J.; Ihee, H.; Jiang, D. *Angew. Chem.* **2008**, *120*, 8958.

(7) Deblase, C. R.; Silberstein, K. E.; Truong, T.-T.; Abruña; Dichtel, W. R. *J. Am. Chem. Soc.* **2013**, *135*, 16821.

(8) Fang, Q.; Wang, J.; Gu, S.; Kaspar, R. B.; Zhuang, Z.; Zheng, J.; Guo, H.; Qiu, S.; Yan, Y. *J. Am. Chem. Soc.* **2015**, *137*, 8352.

(9) Dalapati, S.; Jin, S.; Gao, J.; Xu, Y.; Nagai, A.; Jiang, D. *J. Am. Chem. Soc.* **2013**, *135*, 17310.

(10) (a) Ding, S. Y.; Gao, J.; Wang, Q.; Zhang, Y.; Song, W. G.; Su, C. Y.; Wang, W. *J. Am. Chem. Soc.* **2011**, *133*, 19816. (b) Lin, S.; Diercks, C. S.; Zhang, Y. B.; Kornienko, N.; Nichols, E. M.; Zhao, Y.; Paris, A. R.; Kim, D.; Yang, P.; Yaghi, O. M.; Chang, C. J. *Science* **2015**, *349*, 1208.

(11) (a) Xu, H.; Gao, J.; Jiang, D. *Nat. Chem.* **2015**, *7*, 905. (b) Xu, H.; Chen, X.; Gao, J.; Lin, J.; Addicoat, M.; Irle, S.; Jiang, D. *Chem. Commun.* **2014**, *50*, 1292. (c) Qian, H.; Yang, C.; Yan, X. *Nat. Commun.* **2016**, *7*, 12104.

(12) (a) Seo, J. S.; Whang, D.; Lee, H.; Jun, S. I.; Oh, J.; Jeon, Y. J.; Kim, K. *Nature* **2000**, *404*, 982. (b) Morris, R.; Bu, X. *Nat. Chem.* **2010**, *2*, 353.

(13) Lee, J. Y.; Farha, O. K.; Roberts, J.; Scheidt, K. A.; Nguyen, S. T.; Hupp, J. T. *Chem. Soc. Rev.* **2009**, *38*, 1450.

(14) Budd, P. M.; Ghanem, B. S.; Makhseed, S.; McKeown, N. B.; Msayib, K. J.; Tattershall, C. E. *Chem. Commun.* **2004**, 230.

(15) Colson, J. W.; Dichtel, W. R. *Nat. Chem.* **2013**, *5*, 453.

(16) Kandambeth, S.; Shinde, D. B.; Panda, M. K.; Lukose, B.; Heine, T.; Banerjee, R. *Angew. Chem.* **2013**, *125*, 13290.

(17) (a) Seebach, D.; Beck, A. K.; Heckel, A. *Angew. Chem., Int. Ed.* **2001**, *40*, 92. (b) Pellissier, H. *Tetrahedron* **2008**, *64*, 10279.

(18) Ascherl, L.; Sick, T.; Margraf, J. T.; Lapidus, S. H.; Calik, M.; Hettstedt, C.; Karaghiosoff, K.; Döblinger, M.; Clark, T.; Chapman, K. W.; Auras, F.; Bein, T. *Nat. Chem.* **2016**, *8*, 310.

(19) (a) Biswal, B. P.; Chandra, S.; Kandambeth, S.; Lukose, B.; Heine, T.; Banerjee, R. *J. Am. Chem. Soc.* **2013**, *135*, 5328. (b) Serre, C.; Mellot-Draznieks, C.; Surblé, S.; Audebrand, N.; Filinchuk, Y.; Férey, G. *Science* **2007**, *315*, 1828.

(20) Altava, B.; Burguete, M. I.; Fraile, J. M.; García, J. I.; Luis, S. V.; Mayoral, J. A. M.; Vicent, J. *Angew. Chem., Int. Ed.* **2000**, *39*, 1503.

(21) (a) Heckel, A.; Seebach, D. *Angew. Chem., Int. Ed.* **2000**, *39*, 163. (b) Rheiner, P. B.; Sellner, H.; Seebach, D. *Helv. Chim. Acta* **1997**, *80*, 2027.

(22) The addition of Et_2Zn to cinnamaldehyde catalyzed by TADDOL-POP/Ti afforded the product with only 49% ee.[23]

(23) Wang, X.; Zhang, J.; Liu, Y.; Cui, Y. *Bull. Chem. Soc. Jpn.* **2014**, *87*, 435.

(24) Ma, L.; Falkowski, J. M.; Abney, C.; Lin, W. *Nat. Chem.* **2010**, *2*, 838.

DOI: 10.1021/jacs.6b07714
J. Am. Chem. Soc. 2016, 138, 12332−12335